Acta Crystallographica Section F
Structural Biology and Crystallization Communications
ISSN 1744-3091

Improved crystallization of *Escherichia coli* ATP synthase catalytic complex (F_1) by introducing a phosphomimetic mutation in subunit ε

Ankoor Roy,[a] Marcus L. Hutcheon,[b] Thomas M. Duncan[b]* and Gino Cingolani[a]*

[a]Department of Biochemistry and Molecular Biology, Thomas Jefferson University, Philadelphia, PA 19107, USA, and [b]Department of Biochemistry and Molecular Biology, SUNY Upstate Medical University, Syracuse, NY 13210, USA

Correspondence e-mail: duncant@upstate.edu, gino.cingolani@jefferson.edu

Received 7 July 2012
Accepted 23 August 2012

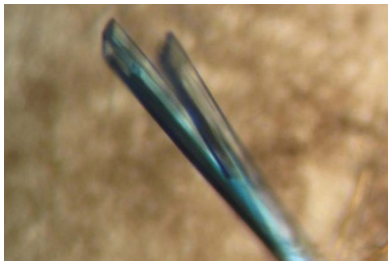

The bacterial ATP synthase (F_OF_1) of *Escherichia coli* has been the prominent model system for genetics, biochemical and more recently single-molecule studies on F-type ATP synthases. With 22 total polypeptide chains (total mass of ~529 kDa), *E. coli* F_OF_1 represents nature's smallest rotary motor, composed of a membrane-embedded proton transporter (F_O) and a peripheral catalytic complex (F_1). The ATPase activity of isolated F_1 is fully expressed by the $\alpha_3\beta_3\gamma$ 'core', whereas single δ and ε subunits are required for structural and functional coupling of *E. coli* F_1 to F_O. In contrast to mitochondrial F_1-ATPases that have been determined to atomic resolution, the bacterial homologues have proven very difficult to crystallize. In this paper, we describe a biochemical strategy that led us to improve the crystallogenesis of the *E. coli* F_1-ATPase catalytic core. Destabilizing the compact conformation of ε's C-terminal domain with a phosphomimetic mutation (εS65D) dramatically increased crystallization success and reproducibility, yielding crystals of *E. coli* F_1 that diffract to ~3.15 Å resolution.

1. Introduction

F-type ATP synthases compose an evolutionarily related family of energy-coupling, ion-transporting enzymes which is responsible for the synthesis of most cellular ATP in plants, animals and many bacteria. The ATP synthase functions as a dual-engine rotary motor (Duncan, 2004). A membrane-embedded complex (F_O, composition $a_1b_2c_{10}$) acts as a turbine to transport protons (H^+; Na^+ in some bacteria). A peripheral stator stalk and a central rotor stalk connect F_O to an extrinsic catalytic complex (F_1, composition $\alpha_3\beta_3\gamma_1\delta_1\varepsilon_1$) in which rotation of the asymmetric central stalk coordinates the conformational changes of three alternating catalytic nucleotide sites during net ATP synthesis or hydrolysis. High-resolution structures of F_1-ATPases have been solved over the past two decades, almost exclusively by crystallographic studies of mitochondrial F_1 (MF_1) isolated from bovine heart (Abrahams *et al.*, 1994; Bowler *et al.*, 2007) or yeast (Kabaleeswaran *et al.*, 2006). Structures of a detergent-solubilized MF_1/*c*-ring complex from yeast (Stock *et al.*, 1999) and bovine heart (Watt *et al.*, 2010) were also determined at medium resolution. On the other hand, the bacterial ATP synthase of *Escherichia coli* (EF_OF_1) has provided the predominant system for genetic and biochemical studies of the functional mechanism of ATP synthases for over 30 years (Gibson, 2000). Likewise, single-molecule studies developed to characterize the rotary mechanics of the enzyme have relied almost exclusively on bacterial enzymes (Noji *et al.*, 2011; Börsch, 2011).

Compared to mitochondrial homologues, bacterial F_1-ATPases have proven very difficult to crystallize and their crystals usually diffract X-rays weakly, to resolutions often not sufficient to build a complete atomic model. For instance, a 4.4 Å map of EF_1 (Hausrath *et al.*, 1999, 2001) computed using 64% complete crystallographic data was reported in 1999. More recently, the structure of *Caldalkalibacillus thermarum* F_1 with all empty nucleotide-binding pockets was reported to 3.3 Å resolution (Stocker *et al.*, 2007). A possible reason for the poorer propensity of bacterial F_1 to crystallize as compared with MF_1 lies in the ε subunit's C-terminal domain (CTD), which, in F_1 of bacteria and chloroplasts, is capable of dynamic conformational changes. Increasing evidence suggests this

Table 1
Summary of diffraction data statistics for EF_1-δ(εS65D).

The numbers in parentheses refer to the statistics for the outer-resolution shell (3.25–3.15 Å).

Crystallization condition	9%(*w*/*v*) PEG 8000, 0.1 *M* MOPS pH 7.0, 100 m*M* $MgSO_4$, 4.0%(*v*/*v*) 1-propanol
Beamline	NSLS X29
Wavelength (Å)	1.075
Space group	*C*2
Reflections (total/unique)	4371954/262052
Unit cell	a = 433.3, b = 181.5, c = 224.2 Å, α = 90.0, β = 108.4, γ = 90.0°
Resolution (Å)	60–3.15
Completeness (%)	91.4 (64.3)
Redundancy	2.6 (2.1)
R_{sym}† (%)	13.9 (76.5)
$\langle I\rangle/\langle\sigma(I)\rangle$	12.4 (2.3)

† $R_{sym} = \sum_{hkl}\sum_i |Ii(hkl) - [I(hkl)]|/\sum_{hkl}\sum_i I_i(hkl)$ where $I_i(hkl)$ is the ith intensity measurement of reflection hkl, including symmetry-related reflections, and $\langle I(hkl)\rangle$ is its average.

'structural plasticity' of ε's CTD serves a regulatory role(s), being modulated by signals from the catalytic sites on F_1 (different nucleotides) and from F_O (proton-motive force, or inhibitor binding to F_O) (Duncan, 2004; Feniouk *et al.*, 2006). Last year, we reported a complete atomic model of EF_1 lacking the δ subunit (EF_1-δ) refined to an $R_{work}/R_{free} \simeq 24.3/26.4\%$, at 3.26 Å resolution (Cingolani & Duncan, 2011). In this structure, the ε-CTD adopts a highly extended conformation which inserts deeply into the central cavity of the enzyme and engages both rotor and stator subunits in extensive contacts that are incompatible with functional rotation. In this paper, we present a strategy to improve the crystallization of EF_1 based on introducing a phosphomimetic mutation in subunit ε.

2. Material and methods

2.1. Cloning, expression and purification of *Escherichia coli* ATP synthase catalytic complex

The genes encoding wild-type EF_OF_1 subunit were cloned in a pUC-based vector pJW1 (Wise, 1990). The εS65D mutation was created by site-directed mutagenesis using the plasmid p3DC (Duncan, Zhou *et al.*, 1995) as a template; DNA sequencing confirmed that εS65D was the only mutation introduced within the *atpDC* genes. Then p3DC+εS65D was cleaved with *Hin*dIII and ligated with a 5.5 kB *Hin*dIII fragment from wild-type p3U (Duncan, Zhou *et al.*, 1995). This p3U+εS65D was used to express EF_OF_1 including the εS65D subunit in *E. coli* strain LE392Δ*atpI-C* (Schaefer *et al.*, 1989). For a typical EF_1 preparation, 10 l of *E. coli* were grown aerobically at 310 K in a Bioflo-2000 fermentor (New Brunswick Scientific) using 10 m*M* glucose and 1%(*v*/*v*) glycerol as carbon sources. Cells were harvested 6–8 h after inoculation and *E. coli* membranes were prepared as described (Duncan, Bulygin *et al.*, 1995). Soluble EF_1 and EF_1(εS65D) were dissociated from membranes and purified at 277 K, as previously described (Senior *et al.*, 1979; Cingolani & Duncan, 2011). Typical yields of purified EF_1 are 50–100 mg per 50 g of wet cells, and specific ATPase activities of 40–45 units mg^{-1} at 303 K under 'routine' conditions (pH 8, 2 m*M* ATP, 1 m*M* Mg acetate), for both wild-type and EF_1(εS65D). The δ subunit was completely removed from EF_1 by gel filtration in the presence of detergent LDAO (lauryldimethylamine oxide) (Hausrath *et al.*, 1999) at room temperature (∼295 K). This procedure provided >80% yield of EF_1-δ. Final samples of purified EF_1-δ and EF_1-δ(εS65D) ($\geq$10 mg ml^{-1}) were quick-frozen in liquid N_2 and stored at 193 K. Protein concentrations were determined by a modified Lowry assay (Peterson, 1977). ATPase activity was assayed at 303 K by a coupled-enzyme assay of ADP produced (Pullman *et al.*, 1960) with typical conditions: 20 m*M* MOPS–Tris [3-(*N*-morpholino)propanesulfonic acid–Tris], pH 8.0, 50 m*M* KCl, 1 m*M* phosphoenol pyruvate, 0.3 m*M* NADH, 0.2 mg pyruvate kinase per ml, 0.1 mg lactate dehydrogenase per ml, 2 m*M* ATP, 1 m*M* magnesium acetate.

2.2. Detection of phosphorylation in subunit ε

Samples of purified EF_1-δ were analysed by SDS–PAGE (Duncan, Bulygin *et al.*, 1995) and stained with SYPRO Orange (Life Technologies); gels were scanned with a Typhoon-9410 imager [GE Healthcare Life Sciences; 488 nm laser, 526 nm short-pass (SP) emission filter] and sample purity was analysed with *ImageQuant TL* software. For detection of putative subunit phosphorylation, SDS–PAGE gels were first stained with Pro-Q Diamond (Life Technologies) and scanned [Typhoon-9410, 532 nm laser, 580 band-pass (BP) emission filter], then stained with SYPRO Orange and scanned for total protein bands as above.

2.3. Crystallization of the ATP synthase catalytic complex (F_1) bearing a phosphomimetic mutation

Prior to crystallization, frozen samples of EF_1-δ(εS65D) at >10 mg ml^{-1} were thawed quickly and extensively dialysed at room temperature against dialysis buffer (50 m*M* Tris–HCl, 0.1 m*M* Na–EDTA, pH 7.5, ±5 m*M* β-mercaptoethanol in a 10 kD cut-off Pierce Slidalyzer (3 ml size). Dialysed EF_1 samples were concentrated to ∼30 mg ml^{-1} by ultrafiltration (Vivaspin, 10 kD cut-off). Crystallization trials were carried out using the hanging-drop vapour diffusion method in Linbro 24-well plates (Hampton Research) in a range of concentrations between 10 and 30 mg ml^{-1}, although the most reproducible and well diffracting crystals were obtained using EF_1-δ at 20 mg ml^{-1}. The most successful crystallization buffer was 0.1 MOPS–NaOH, pH 7.0, $MgSO_4$ 75 to 150 m*M* and PEG 8K, 6–10%(*w*/*v*). Droplets set up by mixing 4 µl of protein with an equal volume of reservoir solution and equilibrated against 600 µl of reservoir solution at 293 K gave the largest EF_1-δ(εS65D) crystals, usually 2–5 d after setting up crystallization. Additives were screened with EF1-δ(εS65D) at a protein concentration of 15 mg ml^{-1} in crystallization buffer; crystallization was carried out by the hanging-drop method in Crystal Quick 96-well plates (Hampton Research) using a HYDRA II crystallization robot, at the Kimmel Cancer Center X-ray Crystallography and Molecular Characterization Shared Resource Facility (Thomas Jefferson University). Concentrated additive (7 µl, typically 1 *M*) was mixed with 53 µl of crystallization buffer (+5 m*M* βME) and 0.4 µl of this mixture was added to 0.4 µl of protein sample.

2.4. X-ray data collection and analysis

Single crystals of EF_1-δ(εS65D) were cryocooled after slow addition of cryoprotectant (glycerol) to 25%(*v*/*v*). Several data sets were collected at National Synchrotron Light Source (NSLS, Upton, NY) beamlines X29 and X6A. Diffraction data were reduced to h, k, l intensities using the programs *DENZO* and *SCALEPACK* (Otwinowski & Minor, 1997) of the *HKL-2000* package. A complete summary of diffraction statistics is presented in Table 1.

3. Results and discussion

3.1. The troublesome crystallogenesis of EF_1-δ

Crystallization of wild-type EF_1-δ was achieved over eight years by a 'brute force' effort that included biochemical procedures and post-crystallization treatments (Cingolani & Duncan, 2011). Several factors were empirically found to promote crystallization. Removing the δ subunit was essential to reduce sample heterogeneity and obtain ordered crystals that diffracted to ∼5–7 Å resolution. Dehydration of EF_1-δ crystals in the presence of glycerol improved diffraction to ∼4.3 Å, greatly reducing the fall-off in diffraction intensity at higher resolution. Finally, addition of ∼1 m*M* AMPPNP (adenyl-imidodiphosphate) during dehydration dramatically improved the diffraction quality and resolution of EF_1-δ crystals. In October 2008, a single, extensively dehydrated crystal was used to collect a complete data set to ∼3.3 Å resolution, at NSLS beamline X25. This crystal belongs to space group *C*2 with unit-cell parameters a = 435.9, b = 183.1, c = 225.4 Å and β = 108.9°, and contains four EF_1-δ complexes in the asymmetric unit. These data were used to determine the structure of the auto-inhibited EF_1-δ, which was refined to an $R_{work}/R_{free} \simeq 24.3/26.4\%$, at 3.26 Å resolution (Cingolani & Duncan, 2011). Despite three years of effort after obtaining this first data set, all attempts to reproduce EF_1-δ crystals diffracting past 3.5 Å resolution were unsuccessful. EF_1-δ crystallization was extremely variable. On average, one dehydrated crystal for every 30–40 tested diffracted past 4 Å resolution, making it difficult to perform co-crystallization studies with other co-factors. Crystallization was also greatly preparation dependent, and even the same EF_1-δ sample that had crystallized in one droplet failed to yield crystals in another drop set up under identical conditions. The success of crystallization could be improved by microseeding of older crystals in solution of freshly purified EF_1-δ, although this still relied on obtaining initial crystals of the enzyme.

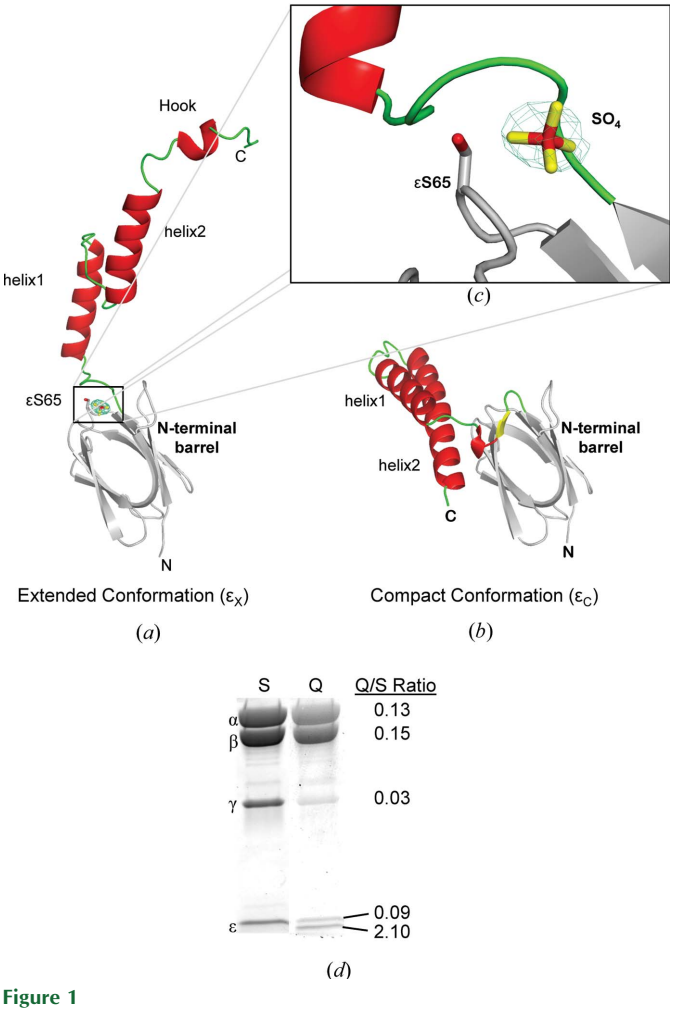

Figure 1
Stabilization of ε-subunit CTD with a phosphomimetic mutation. Ribbon diagrams of ε subunit with the CTD in an extended (pdb 3oaa) (*a*) or compact conformation (*b*) (pdb 1aqt). In both panels, the ε-subunit N-terminal β-barrel (ε1–80) is coloured in grey, while α-helices, β-strands and random coiled regions in ε-CTD are in red, yellow and green, respectively. (*c*) A σ_A-weighted $F_o - F_c$ electron-density map (blue mesh) computed at 3.26 Å resolution is overlaid on the putative ion interpreted as sulfate (SO_4). The density was computed after omitting the ion from the final refined model and is displayed at 5σ above background. The side chain of εS65 coordinating the putative sulfate ion is also shown. The electron-density figure was generated using *PyMOL* (*The PyMOL Molecular Graphics System*, Version 1.5.0.4, Schrödinger, LLC). (*d*) Phosphoprotein staining suggests that a fraction of ε subunit in EF_1 may be phosphorylated. A 20 µg sample of wild-type EF_1-δ was separated on 12.5% SDS–PAGE and subunit bands quantified after first staining with Pro-Q Diamond (phosphoprotein-selective, lane Q), and then after staining total protein with SYPRO Orange (lane S) (see §2). Q/S ratios represent the relative subunit staining intensities for the two dyes. Control samples with phosphorylated and nonphosphorylated proteins (PeppermintStick standards, Life Technologies) were run on the same gel; for a dilution (∼0.07 µg each band) that showed phospho-staining intensities similar to those of the lower ε band of EF_1-δ, Q/S ratios were 2.0 and 5.9 for phosphoprotein standards (ovalbumin and β-casein, respectively), and 0.14 for a nonphosphorylated protein (bovine serum albumin).

3.2. Engineering ε subunit by a phosphomimetic mutation

After determining the structure of EF_1-δ (Cingolani & Duncan, 2011), it became evident that the conformation adopted by ε-CTD was likely the limiting factor in growing reproducibly well diffracting crystals of EF_1-δ. In the structure of EF_1-δ, the ε-CTD adopts a highly extended conformation (denoted as ε_X in Fig. 1*a*), which inserts deeply inside the catalytic F_1 core. This conformation of ε-CTD is drastically different from that seen in the only other bacterial F_1 structure determined so far (Stocker *et al.*, 2007) and in all structures of isolated bacterial ε (Wilkens & Capaldi, 1998; Uhlin *et al.*, 1997; Yagi *et al.*, 2007), in which ε-CTD folds as a compact helical hairpin (denoted as ε_C in Fig. 1*b*). Likewise, ε-CTD is also compact in ε subunits of all mitochondrial homologues, due to a mitochondria-specific subunit that stabilizes the ε_C state (Gibbons *et al.*, 2000; Kabaleeswaran *et al.*, 2006). Thus, we hypothesized that the co-existence of inhibitory (ε_X) and noninhibitory (ε_C) conformations of ε-CTD in EF_1-δ samples could be the intrinsic source of heterogeneity hampering reproducible crystallization. In an attempt to optimize both the success rate and reproducibility of EF_1-δ crystallization, we focused on an unexpected feature revealed by the EF_1-δ structure. In the crystal structure, a 4–8σ peak of positive density was seen coordinating the hydroxyl group of Ser65 in ε (εS65); this site was originally modelled as a sulfate ion (Fig. 1*c*) (Cingolani & Duncan, 2011). This putative ion is located at hydrogen-bonding distance from the εS65 hydroxyl group and would sterically hinder conversion to the ε_C conformation: superimposing the ε_X and ε_C conformations using the ε-NTD (N-terminal domain), it was found that this density would clash with atoms of Thr82, Ala83 and Ile84, which move to become part of the ε-NTD β-barrel in the ε_C state (Fig. 1*b*, yellow strand). We hypothesized that this ion or possible phosphorylation of εS65 would destabilize the ε_C state, thus favouring the inhibitory ε_X state. In support of this hypothesis, selective staining of purified EF_1-δ with Pro-Q Diamond Phosphoprotein Gel Stain suggests that a fraction of ε subunit is phosphorylated (Fig. 1*d*), although amounts recovered from bands were insufficient to confirm this by mass spectrometry. Therefore, to mimic the ion or possible phosphorylation at εS65 and increase occupancy of the ε_X state in

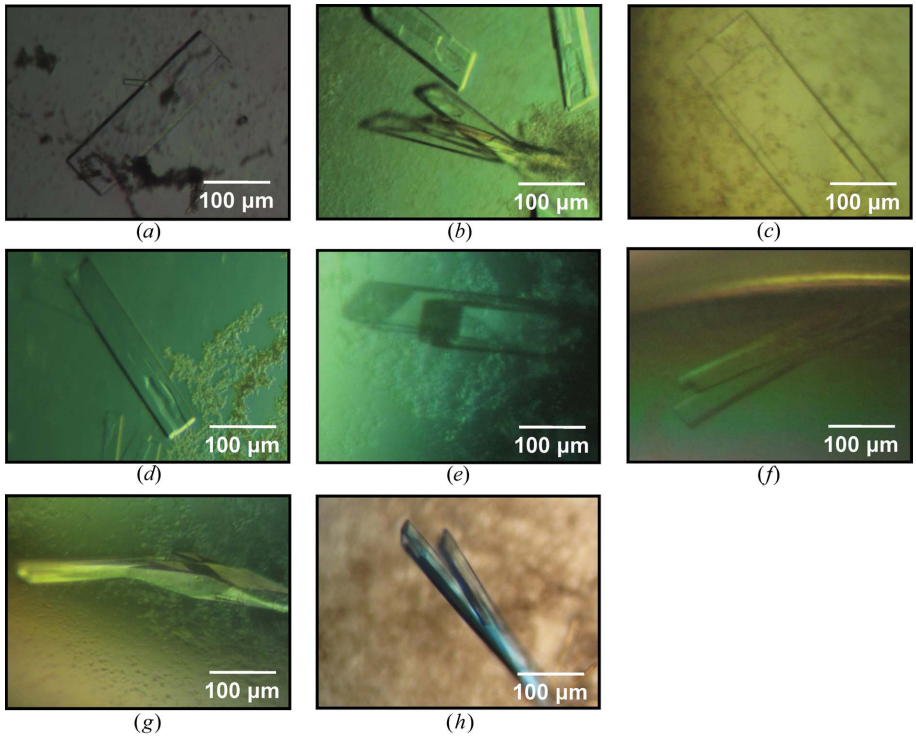

Figure 2
Effects of additives on crystallization of EF_1-δ. (*a*), (*b*) Representative crystals of EF_1-δ(εS65D) obtained by the hanging-drop vapour diffusion method using microseeding. Crystals obtained (without seeding) in the presence of 4.0%(*v*/*v*) of 1-propanol (*c*), (*d*), acetone (*e*), (*f*), or 1-butanol (*g*), (*h*).

EF_1-δ samples, we replaced εS65 with an aspartic acid, whose carboxyl group serves as a phosphomimetic.

3.3. Crystallization of EF_1-δ(εS65D)

EF_1-δ(εS65D) was expressed and purified as for the wild-type enzyme. In crystallization trials, EF_1-δ(εS65D) had dramatically greater success of crystallization. Large plate-like crystals could be obtained reproducibly within 36–48 h in the presence of 9–11%(*w*/*v*) PEG 8K, 150 m*M* $MgSO_4$, 0.1 *M* MOPS–NaOH, pH 7.0. In contrast to EF_1-δ, microseeding did not significantly improve crystallogenesis, and crystals obtained without microseeding (Figs. 2*a* and 2*b*) were larger than those previously obtained with wild-type EF_1-δ. The success of EF_1-δ(εS65D) crystallization was close to 90%, with nearly every drop showing large rod-like crystals. The ability to reliably obtain crystals allowed us to screen crystallization additives. Several compounds were found to increase the size of EF_1-δ(εS65D) crystals and reduce clustering when used at $\geq$4%(*v*/*v*) final concentration. The most significant and reproducible were 1-propanol (Figs. 2*c* and 2*d*), acetone (Figs. 2*e* and 2*f*) and 1-butanol (Figs. 2*g* and 2*h*). In diffraction trials, most EF_1-δ(εS65D) diffracted X-rays to $\sim$5 Å resolution even without dehydration. Dehydration in the presence of nucleotide dramatically improved diffraction quality and reduced radiation-induced diffraction decay. In a screen of $\sim$20 dehydrated crystals at NSLS beamline X29, a few EF_1-δ(εS65D) surpassed 3.5 Å resolution. A complete data set to 3.15 Å resolution was measured at beamline X29 (Table 1), and subsequent diffraction analysis revealed this crystal form belongs to space group *C*2 with four EF_1-δ(εS65D) in the crystallographic asymmetric unit, corresponding to 32 polypeptide chains and approximately 13 250 residues. Although the best diffraction data recorded from EF_1-δ(εS65D) crystals were slightly improved in resolution as compared to wild-type EF_1-δ crystals (3.15 *versus* 3.26 Å), the reproducibility of EF_1-δ(εS65D) crystals was dramatically enhanced. More consistent growth of EF_1-δ(εS65D) crystals, additional refinement of additives and dehydration procedures should help us achieve higher-resolution structures in the future.

We are grateful to the staff at NSLS beamlines X29 and X6A. We thank Nancy Walker-Kopp for technical assistance. This work was supported by the US National Institutes of Health (grant No. R01GM083088).

References

Abrahams, J. P., Leslie, A. G., Lutter, R. & Walker, J. E. (1994). *Nature (London)*, **370**, 621–628.
Börsch, M. (2011). *Biol. Chem.* **392**, 135–142.
Bowler, M. W., Montgomery, M. G., Leslie, A. G. & Walker, J. E. (2007). *J. Biol. Chem.* **282**, 14238–14242.
Cingolani, G. & Duncan, T. M. (2011). *Nat. Struct. Mol. Biol.* **18**, 701–707.
Duncan, T. M. (2004). *The Enzymes*, Vol. 23, *Energy Coupling and Molecular Motors*, edited by D. D. Hackney & F. Tamanoi, pp. 203–275. New York: Academic Press.
Duncan, T. M., Bulygin, V. V., Zhou, Y., Hutcheon, M. L. & Cross, R. L. (1995). *Proc. Natl Acad. Sci. USA*, **92**, 10964–10968.
Duncan, T. M., Zhou, Y., Bulygin, V. V., Hutcheon, M. L. & Cross, R. L. (1995). *Biochem. Soc. Trans.* **23**, 736–741.
Feniouk, B. A., Suzuki, T. & Yoshida, M. (2006). *Biochim. Biophys. Acta*, **1757**, 326–338.
Gibbons, C., Montgomery, M. G., Leslie, A. G. & Walker, J. E. (2000). *Nat. Struct. Biol.* **7**, 1055–1061.
Gibson, F. (2000). *Trends Biochem. Sci.* **25**, 342–344.
Hausrath, A. C., Capaldi, R. A. & Matthews, B. W. (2001). *J. Biol. Chem.* **276**, 47227–47232.
Hausrath, A. C., Grüber, G., Matthews, B. W. & Capaldi, R. A. (1999). *Proc. Natl Acad. Sci. USA*, **96**, 13697–13702.

Kabaleeswaran, V., Puri, N., Walker, J. E., Leslie, A. G. & Mueller, D. M. (2006). *EMBO J.* **25**, 5433–5442.
Noji, H., Okuno, D. & Ikeda, T. (2011). *Chem. Sci.* **2**, 2086–2093.
Otwinowski, Z. & Minor, W. (1997). *Methods Enzymol.* **276**, 307–326.
Peterson, G. L. (1977). *Anal. Biochem.* **83**, 346–356.
Pullman, M. E., Penefsky, H. S., Datta, A. & Racker, E. (1960). *J. Biol. Chem.* **235**, 3322–3329.
Schaefer, E. M., Hartz, D., Gold, L. & Simoni, R. D. (1989). *J. Bacteriol.* **171**, 3901–3908.
Senior, A. E., Fayle, D. R., Downie, J. A., Gibson, F. & Cox, G. B. (1979). *Biochem. J.* **180**, 111–118.
Stock, D., Leslie, A. G. & Walker, J. E. (1999). *Science*, **286**, 1700–1705.
Stocker, A., Keis, S., Vonck, J., Cook, G. M. & Dimroth, P. (2007). *Structure*, **15**, 904–914.
Uhlin, U., Cox, G. B. & Guss, J. M. (1997). *Structure*, **5**, 1219–1230.
Watt, I. N., Montgomery, M. G., Runswick, M. J., Leslie, A. G. & Walker, J. E. (2010). *Proc. Natl Acad. Sci. USA*, **107**, 16823–16827.
Wilkens, S. & Capaldi, R. A. (1998). *J. Biol. Chem.* **273**, 26645–26651.
Wise, J. G. (1990). *J. Biol. Chem.* **265**, 10403–10409.
Yagi, H., Kajiwara, N., Tanaka, H., Tsukihara, T., Kato-Yamada, Y., Yoshida, M. & Akutsu, H. (2007). *Proc. Natl Acad. Sci. USA*, **104**, 11233–11238.